Journal of the Ceramic Society of Japan 116 [1] 137-140 2008 Paper

Effects of impurities on formation pores during solidification for porous alumina and its compressive strength

Shunkichi UENO, Li M. LIN, Hideo NAKAJIMA and Eiichi YASUDA*

The Institute of Scientific and Industrial Research, Osaka University, 8-1, Mihogaoka, Ibaraki, Osaka 567-0047
***Materials and Structure Laboratory, Tokyo Institute of Technology, 4259, Nagatsuta, Midori-ku, Yokohama 226-8503**

Porous alumina with glassy boundary phase consisting of with silica and calcia components was fabricated by unidirectional solidification under pressurized hydrogen atmosphere using alumina feed rod with silica and calcia additives. The pores were elongated along the solidification direction. The glassy boundary phase was directly introduced in the solidified sample during the solidification. The porosity and pores size decrease with increasing total pressure. When a high purity alumina feed rod was used for the solidification, no glassy boundary phase was formed on the grain boundary and the grain boundary cracks in the porous alumina were observed. For comparison, non-porous alumina samples were fabricated by unidirectional solidification in Ar atmosphere using alumina feed rods with and without the additives. The former sample with the additives possesses a boundary phase, while the grain boundary cracks were formed in latter sample. The compressive strengths of non-porous solidified alumina samples with and without boundary glassy phase were 1679 and 267 MPa, respectively; that with boundary phase slightly increased by a heat treatment at 1600°C. The compressive strength of porous alumina with 25.9% porosity was 512 MPa which is larger than that of non-porous alumina without glassy boundary phase. The compressive strength of unidirectionally solidified alumina samples were improved by formation of glassy boundary phase at their grain boundary.

Key-words : Unidirectional solidification, Porous alumina, Glassy boundary phase

[Received August 27, 2007; Accepted November 15, 2007]

1. Introduction

Porous oxide ceramics have been used as hot gas or molten metal filters and catalyst carriers because of their excellent mechanical properties, high temperature resistance, and chemical stabilities.[1),2)] In the application of macro-porous ceramics for filters, control of porous structure such as pore shape, porosity, and pore size is an important issue in the fabrication process. Several research groups developed porous alumina with directional pores by sintering methods.[3)-5)] In their methods, since the porous alumina with directional pores are obtained via sintering process, it is difficult to control the pore diameter. The present authors proposed a new fabrication method for porous alumina with directional cylindrical pores by unidirectional solidification under pressurized hydrogen atmosphere.[6)] In this method, the porous structure was formed at solid-liquid interface according to hydrogen gas solubility gap between solid and liquid phases during the solidification; the porosity and pore size can be controlled by ambient total pressure and hydrogen partial pressure.[6)] Furthermore, it was reported that the porosity in the unidirectionally solidified porous alumina increases with increasing silica content in the feed rod.[7)] These results suggest that pores formation mechanism can be explained by not only hydrogen gas solubility gap between solid and liquid phases, but also vaporization of silica component in the liquid phase.

For the application of porous alumina with cylindrical pores for filters, it is important not only to control porous structure during fabrication process but also to give mechanical properties of the sample. The mechanical properties of ceramics are sensitive to the amount, component, and structure of boundary phase. Since irresolvable impurity elements for the solid phase are eliminated from the solid phase during the solidification by segregation, it is expected that the irresolvable impurities build up a glassy boundary phase at the grains boundary. It is known that when high purity oxide feed rod is used for the solidification, no boundary phase is formed at the boundary.[8)] Hence, it is easy to predict that a polycrystalline monolithic solidified oxide is brittle. However, it is possible to control the formation of boundary phase during the solidification by adding a large amount of impurity phases in the feed rod.

In the present work of porous alumina with directional pores by unidirectional solidification using a feed rod with silica and calcia additives was fabricated in order to discuss the formation mechanism of pores and in-situ formation mechanism of glassy boundary phase during the unidirectional solidification. Compressive strength of the unidirectionally solidified porous and non-porous alumina with and without glassy boundary phase is also examined.

2. Experimental procedures

For the preparation of feed rod, high purity alumina (99.99% purity, Sumitomo Chemical Co., Ltd.), silica (99.9% purity, Admatechs Co., Ltd.), and calcia (99.9% purity, Ube Material Industries Ltd.) powders were used as starting materials. The powders were mixed with a binder in water and a green rod was prepared by slip casting method. After drying in air, calcination was performed at 1200°C for 2 h in air and then, the feed rod with 8 mm diameter and 150 mm length was prepared.

The solidification was performed using optical floating zone apparatus under pressurized hydrogen gas. 100%H_2 gas, 50%H_2–Ar mixed gas, or 10%H_2–Ar mixed gas were used in the present work. The total pressure was controlled in the range from 0.2 MPa to 0.8 MPa. As shown in **Fig. 1**,

xenon lamp was used as a heating source. The xenon lamp and melting zone put on the focus in the elliptical mirror. The feed rod was hooked on upper shaft and another feed rod was fixed with lower shaft. This melting system was set up in a quartz tube. The environmental gas was introduced into quartz tube. The transference velocity of the floating zone was fixed to 200 mm/h in the present work.

The transversal and longitudinal cross-sections of the samples against the solidification direction were observed by SEM (JEOL JSM-6360T). The porosity of the samples was calculated from ratio of the area of pores and bulk (A_{pore}/A_{bulk}, A_{pore} and A_{bulk} denote the area of pores and bulk) using whole of the transversal cross section images. The average pore diameter was calculated from the equivalent setting pore diameter for each pore ($\sum d_i/n$, d_i and n denote equivalent setting pore diameter for each pore and number of pores).

Since the boundary phase was formed in less time during the solidification process, a heat treatment was performed at 1600°C for 2 h in air for stabilization of the grains boundary.

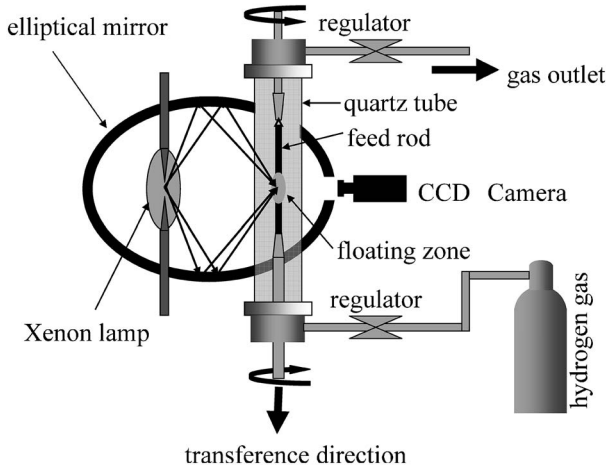

Fig. 1. Optical floating zone furnace used in the present study.

The compressive strength tests for the samples were performed according to JIS-R1608 using universal testing machine (Shimazu-200t Hydraulic System Universal Testing Machine). Cylindrical shape samples with approximately diameter $\phi = 8$ mm and height t = 10 mm are used for the test. The direction of the cylindrical pores is parallel to the stress application direction. The diameter and height of the samples were measured exactly and then, the compressive strength σ_c was calculated by Eq. (1),

$$\sigma_c = \frac{4P}{\pi d^2} \quad (1)$$

where P and d denote the ultimate load for crush and the diameter of the sample, respectively.

3. Results and discussion

Since the melting point of calcia and silica complex oxides are lower than that of alumina, these phases are used as additives for formation of boundary phase in solidified alumina during the solidification. In the present experiment, the composition of the feed rod was fixed to Al_2O_3 : SiO_2 : CaO = 82.6 : 16.5 : 0.9 in molar ratio.

Figure 2 shows the transversal cross section views of the samples as a function of the pressure of hydrogen or mixed gas. The porosity and pore size decreases with increasing total pressure and increases with increasing hydrogen partial pressure. Similar tendency can be found in the result of our previous report, where high purity alumina feed rod was used for the solidification.[6] **Figure 3** shows the porosity of the samples prepared in 50%H_2-50%Ar atmosphere under various pressure. The porosity of the solidified alumina increased with increasing silica content in the feed rod as shown in our previous report.[7] Hence, it is considered that there are two different kinds of mechanisms for formation of pores in the present study, i.e. (1) pores are formed at solid-liquid interface due to hydrogen gas solubility gap at the melting point as reported previoiusly[6] and (2) pores are formed by vaporization of silica component in the liquid

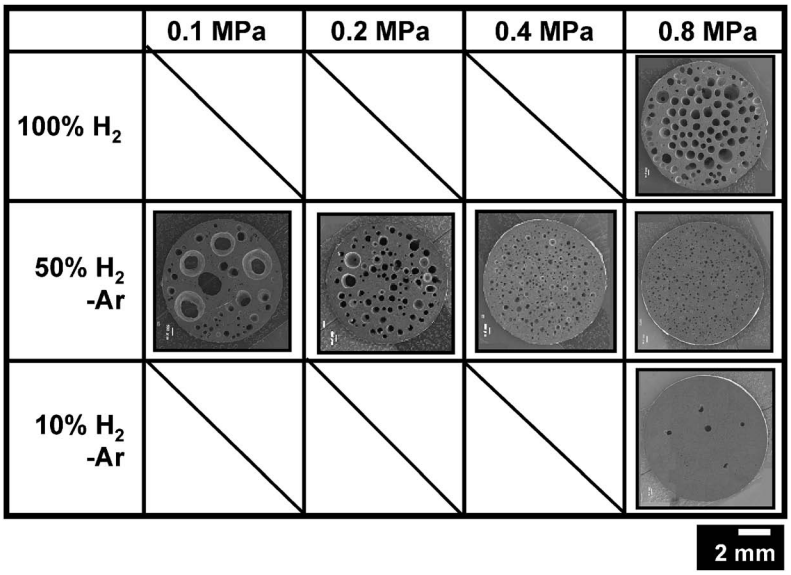

Fig. 2. Transversal cross section views of solidified porous alumina.

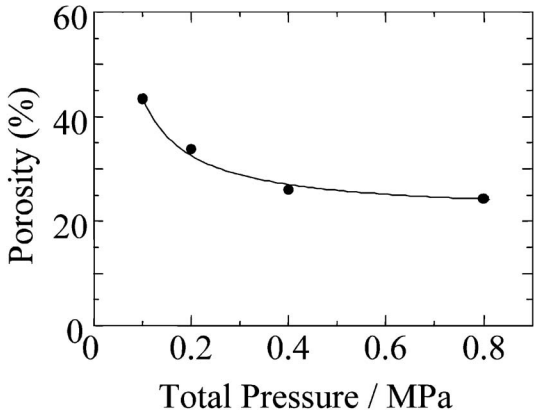

Fig. 3. Porosity of the samples prepared in 50%H_2–50%Ar atmosphere under various pressure.

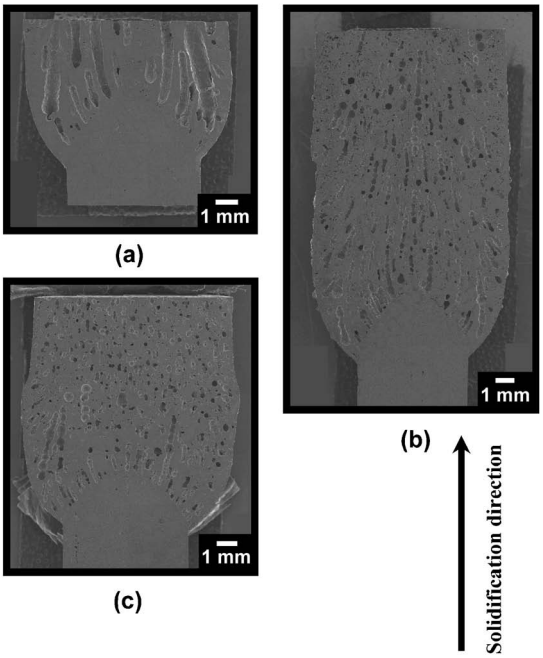

Fig. 4. Longitudinal cross section views of the samples prepared under 50%H_2–50%Ar atmosphere at (a) 0.2, (b) 0.4, and (c) 0.8 MPa, respectively.

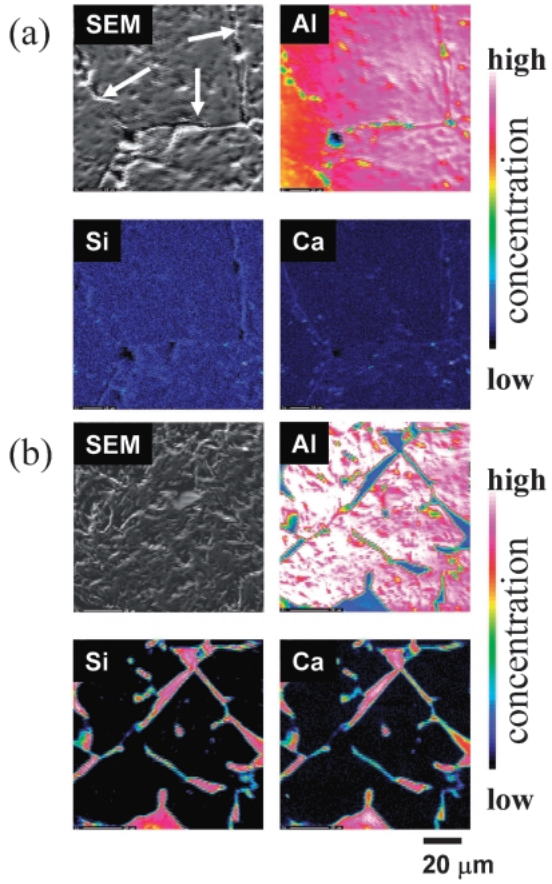

Fig. 5. Results of EPMA analysis for non-porous solidified samples prepared using (a) high purity alumina feed rod and (b) feed rod added with silica and calcia, respectively. The boundary phase in (b) is consisted with silicon-calcium oxides.

phase and trapping the gas bubbles by the solid phase as reported previously.[7] Since the pores are formed at solid-liquid interface during the unidirectional solidification in both cases, the pressure of pores at solid-liquid interface are balanced with environmental total pressure. Hence, the porosity decreases with increasing total pressure according to Boyles's law regardless of the formation mechanism of pores.

Figures 4(a), (b) and (c) show the longitudinal cross section views of the samples prepared under 50%H_2–50%Ar atmosphere at 0.2, 0.4, and 0.8 MPa, respectively. It can be seen that cylindrical pores are aligned in the solidification direction in these samples. However, the length of pore decreases with increasing total pressure. From the figures, it is confirmed that the number of pores increases with increasing total pressure. These results suggest that the number of nucleation sites of pores increases with increasing total pressure. Since a non-porous sample was obtained under Ar atmosphere using silica and calcia added feed rod, the vaporization of silica component is caused by a reaction of silica with hydrogen in the liquid phase. The hydrogen gas solubility into the liquid phase increases with increasing hydrogen gas partial pressure according to Sieverts' law as reported previously.[6] Hence, it is considered that the number of nucleation site of pores increases with increasing hydrogen gas solubility in the liquid phase.

Figures 5(a) and (b) show the result of EPMA analysis for non-porous solidified samples prepared using high purity alumina feed rod and feed rod added with silica and calcia, respectively. These images were obtained from transversal cross section of the samples. In Fig. 5(a), some grain boundaries were observed in the SEM image as indicated by arrows. However, no evidence for boundary phase was obtained from this figure. In this case, the boundary is a kind of cracks. On the other hand, no clear grain boundary was found in SEM image in Fig. 5(b). However, the EPMA analysis shows that a boundary phase with silica and calcia components was formed for the sample of feed rod added with silica and calcia. This grain boundary was considered to be directly introduced in the sample during the solidification.

Figure 6 shows powder X-ray diffraction patterns of the

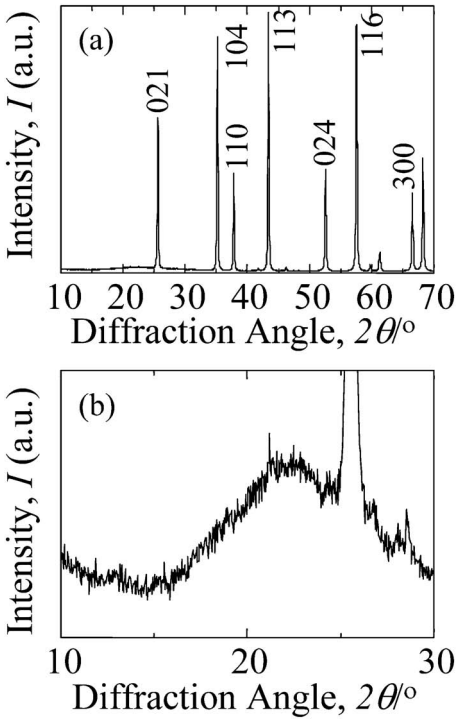

Fig. 6. Powder X-ray diffraction pattern of the sample prepared using feed rod added with silica and calcia. (a) All peaks can be indexed as α-alumina phase. (b) A hallo pattern is observed in 2θ rage from 15 to 30°.

Table 1. Compressive Strength of Non-porous and Porous Solidified Alumina

Sample	porosity (%)	feed rod	compressive strength (MPa)
non-porous alumina	0	high purity alumina	267.2 ± 86.2
non-porous alumina after heat treatment	0	high purity alumina	251.1 ± 104.1
non-porous alumina	0	20%SiO_2-1%CaO added alumina	1678.8 ± 38.1
non-porous alumina after heat treatment	0	20%SiO_2-1%CaO added alumina	1875.4 ± 123.8
porous alumina	25.9	20%SiO_2-1%CaO added alumina	512.0 ± 97.6

sample prepared using feed rod added with silica and calcia. All peaks in Fig. 6(a) can be indexed as corundum phase. Fig. 6(b) shows a magnified pattern of (a) in the 2θ range from 10 to 30°. A hallo pattern can be observed between $2\theta = 15$ and 30° which is well known pattern due to existence of silicate amorphous phase. Hence, it is recognized that the boundary phase found in Fig. 5(b) is a glassy phase which is consisted with silica and calcia components.

The compressive strength of non-porous and porous solidified samples is summarized in **Table 1**. The number of measurements test for each sample was three. The compressive strength of non-porous samples prepared using high purity alumina feed rod and feed rod added with silica and calcia are 267 and 1679 MPa, respectively. Since the former sample has many cracks, the compressive strength of this sample is very low. On the other hand, since the latter sample has glassy boundary phase without cracks, the compressive strength of this sample is 6 times larger than that of the former sample. The compressive strength of porous sample with 25.9% porosity which prepared under 50%H_2–50%Ar atmosphere at 0.4 MPa using feed rod added with silica and calcia is 512 MPa. Since a small amount of silica component vaporizes during the solidification process, the composition of the boundary glassy phase may be slightly different from that of non-porous sample. However, the compressive strength of the solidified porous alumina can be improved by adding silica and calcia component in the feed rod. The non-porous alumina prepared using high purity alumina feed rod has no boundary phase at the grain boundary hence no glassy boundary phase is formed by the heat treatment. On the other hand, the strength for the sample with glassy boundary phase slightly improved by the heat treatment. Since the melting points of the silica-calcia binary compounds are lower than 1600°C, such enhancement is attributed to the bonding of grains in the boundary phase due to the heat treatment.

4. Conclusion

A porous alumina with cylindrical pores can be fabricated by unidirectional solidification under pressurized hydrogen atmosphere using alumina feed rod with silica and calcia additives. A glassy boundary phase which is consisted with silica and calcia components is directly introduced in the solidified alumina sample during the solidification. Many cracks are induced in the solidified alumina sample when a high purity alumina feed rod is used for the solidification. The compressive strength of the solidified alumina is improved by the glassy boundary phase. The compressive strength of non-porous solidified alumina with the glassy phase is six times larger than that of non-porous solidified alumina without grassy boundary phase.

Acknowledgements This work was supported by the Grant-in-Aid for Scientific Research (C) (No. 18560655) by the Japan Society for the Promotion of Science. The compressive test was performed at Tokyo Institute of Technology on Collaborative Research Project of Materials and Structure Laboratory.

References

1) R. W. Rice, "Porosity of Ceramics," Marcel Decker, New York (1998).
2) K. Ishizaki, S. Komarneni and M. Nanko, "Porous Materials: Process Technology and Applications, Materials Technology Series," Kluwer Academic Publishers (1998).
3) G. J. Zhang, J. F. Yang and T. Ohji, *J. Am. Ceram. Soc.*, 84, 1395–97 (2001).
4) T. Isobe, T. Tomita, Y. Kameshima, A. Nakajima and K. Okada, *J. Eur. Ceram. Soc.*, 26, 957–960 (2006).
5) T. Fukasawa, Z. Y. Deng, M. Ando and T. Ohji, *J. Ceram. Soc. Japan*, 109, 1035–1038 (2001).
6) S. Ueno, L. M. Lin and H. Nakajima, *J. Am. Ceram. Soc.*, in press.
7) S. Ueno, L. M. Lin and H. Nakajima, *Adv. Sci. Technol.*, 45–53, 799–802 (2006).
8) Y. Waku, N. Nakagawa, T. Wakamoto, H. Ohtsubo, K. Shimizu and Y. Kohtoku, *J. Mater. Sci.*, 33, 1217–1225 (1998).